A Glucosinolate Metabolism Pathway in Living Plant Cells Mediates Broad-Spectrum Antifungal Defense

Pawel Bednarek, *et al.*

4. L. Gomez-Gomez, T. Boller, *Trends Plant Sci.* **7**, 251 (2002).
5. T. Nürnberger, B. Kemmerling, *Trends Plant Sci.* **11**, 519 (2006).
6. C. Denoux *et al.*, *Mol. Plant* **1**, 423 (2008).
7. B. A. Halkier, J. Gershenzon, *Annu. Rev. Plant Biol.* **57**, 303 (2006).
8. K. F. M.-J. Tierens *et al.*, *Plant Physiol.* **125**, 1688 (2001).
9. M. S. C. Pedras, Q.-A. Zheng, R. S. Gadagi, *Chem. Commun. (Camb.)* 368 (2007).
10. W. Songnuan *et al.*, in *Biology of Plant-Microbe Interactions*, M. Lorito, S. L. Loo, F. Scala, Eds. (International Society for Molecular Plant-Microbe Interactions, St. Paul, MN, 2008), vol. 6.
11. L. Gomez-Gomez, T. Boller, *Mol. Cell* **5**, 1003 (2000).
12. M. T. Nishimura *et al.*, *Science* **301**, 969 (2003).
13. A. Heese *et al.*, *Proc. Natl. Acad. Sci. U.S.A.* **104**, 12217 (2007).
14. D. Chinchilla *et al.*, *Nature* **448**, 497 (2007).
15. G. E. Schaller, A. B. Bleecker, *Science* **270**, 1809 (1995).
16. J. M. Alonso, T. Hirayama, G. Roman, S. Nourizadeh, J. R. Ecker, *Science* **284**, 2148 (1999).
17. T. Gigolashvili *et al.*, *Plant J.* **50**, 886 (2007).
18. J. L. Celenza *et al.*, *Plant Physiol.* **137**, 253 (2005).
19. K. K. Niyogi, G. R. Fink, *Plant Cell* **4**, 721 (1992).
20. A. N. Stepanova, J. M. Hoyt, A. A. Hamilton, J. M. Alonso, *Plant Cell* **17**, 2230 (2005).
21. Y. Zhao *et al.*, *Genes Dev.* **16**, 3100 (2002).
22. G. W. Haughn, L. Davin, M. Giblin, E. W. Underhill, *Plant Physiol.* **97**, 217 (1991).
23. J. H. Kim, T. P. Durrett, R. L. Last, G. Jander, *Plant Mol. Biol.* **54**, 671 (2004).
24. M. R. Hemm, M. O. Ruegger, C. Chapple, *Plant Cell* **15**, 179 (2003).
25. T. Gigolashvili, R. Yatusevich, B. Berger, C. Müller, U.-I. Flügge, *Plant J.* **51**, 247 (2007).
26. M. Y. Hirai *et al.*, *Proc. Natl. Acad. Sci. U.S.A.* **104**, 6478 (2007).
27. I. E. Sønderby *et al.*, *PLoS One* **2**, e1322 (2007).
28. E. R. Radwanski, A. J. Barczak, R. L. Last, *Mol. Gen. Genet.* **253**, 353 (1996).
29. M. Nafisi *et al.*, *Plant Cell* **19**, 2039 (2007).
30. R. Schuhegger *et al.*, *Plant Physiol.* **141**, 1248 (2006).
31. W. P. Burmeister, S. Cottaz, P. Rollin, A. Vasella, B. Henrissat, *J. Biol. Chem.* **275**, 39385 (2000).
32. P. L. Conklin, S. A. Saracco, S. R. Norris, R. L. Last, *Genetics* **154**, 847 (2000).
33. C. Barth, G. Jander, *Plant J.* **46**, 549 (2006).
34. N. C. Collins *et al.*, *Nature* **425**, 973 (2003).
35. V. Lipka *et al.*, *Science* **310**, 1180 (2005).
36. P. Bednarek *et al.*, *Science* **323**, 101 (2009).
37. W. A.M. et al, *PLoS Genet.* **3**, 1687 (2007).
38. V. Lambrix, M. Reichelt, T. Mitchell-Olds, D. J. Kliebenstein, J. Gershenzon, *Plant Cell* **13**, 2793 (2001).
39. Z. Zhang, J. A. Ober, D. J. Kliebenstein, *Plant Cell* **18**, 1524 (2006).
40. A. M. Wentzell, D. J. Kliebenstein, *Plant Physiol.* **147**, 415 (2008).
41. K. Schlaeppi, N. Bodenhausen, A. Buchala, F. Mauch, P. Reymond, *Plant J.* **55**, 774 (2008).
42. V. Parisy *et al.*, *Plant J.* **49**, 159 (2007).
43. R. Howden, C. R. Andersen, P. B. Goldsbrough, C. S. Cobbett, *Plant Physiol.* **107**, 1067 (1995).
44. E. Grill, S. Löffler, E. L. Winnacker, M. H. Zenk, *Proc. Natl. Acad. Sci. U.S.A.* **86**, 6838 (1989).
45. R. Howden, C. S. Cobbett, *Plant Physiol.* **100**, 100 (1992).
46. D. F. Ortiz, T. Ruscitti, K. F. McCue, D. W. Ow, *J. Biol. Chem.* **270**, 4721 (1995).
47. Z. S. Li *et al.*, *Proc. Natl. Acad. Sci. U.S.A.* **94**, 42 (1997).
48. P. A. Rea, Z. S. Li, Y. P. Lu, Y. M. Drozdowicz, E. Martinoia, *Annu. Rev. Plant Physiol. Plant Mol. Biol.* **49**, 727 (1998).
49. M. Stein *et al.*, *Plant Cell* **18**, 731 (2006).
50. Y. Kobae *et al.*, *Plant Cell Physiol.* **47**, 309 (2006).
51. D.-Y. Kim, L. Bovet, M. Maeshima, E. Martinola, Y. Lee, *Plant J.* **50**, 207 (2007).
52. S. Debroy, R. Thilmony, Y. B. Kwack, K. Nomura, S. Y. He, *Proc. Natl. Acad. Sci. U.S.A.* **101**, 9927 (2004).
53. S. Uknes *et al.*, *Plant Cell* **4**, 645 (1992).
54. A.-C. Cazalé, S. Clemens, *FEBS Lett.* **507**, 215 (2001).
55. M. G. Kim *et al.*, *Cell* **121**, 749 (2005).
56. P. Hauck, R. Thilmony, S. Y. He, *Proc. Natl. Acad. Sci. U.S.A.* **100**, 8577 (2003).
57. N. Beaudoin, C. Serizet, F. Gosti, J. Giraudat, *Plant Cell* **12**, 1103 (2000).
58. M. Ghassemian *et al.*, *Plant Cell* **12**, 1117 (2000).
59. G. Brader, E. Tas, E. T. Palva, *Plant Physiol.* **126**, 849 (2001).
60. D. J. Kliebenstein, A. Figuth, T. Mitchell-Olds, *Genetics* **161**, 1685 (2002).
61. M. D. Mikkelsen *et al.*, *Plant Physiol.* **131**, 298 (2003).
62. We thank S. Abel for *ugt74B1-2*; J. L. Celenza for *atr1-3, atr4-1/cyp83B1, cyp79B2 cyp79B3*, and *trp3-1*; C. S. Cobbett for *cad1-3/pcs1* and *cad2-1/gsh1*; P.L. Conklin for *vtc1-1* and *vtc2-1*; R. Blum for *pcs1-1, pcs2-1*, and *pcs1-1 pcs2-1*; S. C. Somerville for *pcs1-2*; and Arabidopsis Biological Resource Center for insertion lines. Ph.D. stipend support to N.K.C. comes from NIH National Research Service Award–Kirschstein Postdoctoral Fellowship. Support to A.M.A. and G.J. comes from NSF grants IOS-0718733 and DBI-0500550. Support to F.M.A. comes from NSF grant MCB-0519898 and NIH grant R37-GM48707.

A Glucosinolate Metabolism Pathway in Living Plant Cells Mediates Broad-Spectrum Antifungal Defense

Paweł Bednarek,[1]* Mariola Piślewska-Bednarek,[1] Aleš Svatoš,[2] Bernd Schneider,[2] Jan Doubský,[2] Madina Mansurova,[2]† Matt Humphry,[1] Chiara Consonni,[1] Ralph Panstruga,[1] Andrea Sanchez-Vallet,[3] Antonio Molina,[3] Paul Schulze-Lefert[1]*

Selection pressure exerted by insects and microorganisms shapes the diversity of plant secondary metabolites. We identified a metabolic pathway for glucosinolates, known insect deterrents, that differs from the pathway activated by chewing insects. This pathway is active in living plant cells, may contribute to glucosinolate turnover, and has been recruited for broad-spectrum antifungal defense responses. The *Arabidopsis CYP81F2* gene encodes a P450 monooxygenase that is essential for the pathogen-induced accumulation of 4-methoxyindol-3-ylmethylglucosinolate, which in turn is activated by the atypical PEN2 myrosinase (a type of β-thioglucoside glucohydrolase) for antifungal defense. We propose that reiterated enzymatic cycles, controlling the generation of toxic molecules and their detoxification, enable the recruitment of glucosinolates in defense responses.

Flowering plants synthesize and accumulate a vast array of structurally diversified small molecules known as secondary metabolites (*1*). Each particular compound class is usually restricted to a narrow phylogenetic lineage, the result of genetic adaptations enabling or restricting interactions with other organisms. Although the chemical diversification of several secondary metabolite classes is driven by microbes and in-

sects (*1*), it is often difficult to prove their presumed antimicrobial or insect-deterring functions in a whole-organism context. Among the notable exceptions are camalexin, an inducible *Arabidopsis* antimicrobial (phytoalexin) (*2*) and glucosinolates (Fig. 1A), Capparales-specific (which includes the Brassicaceae) thio-glucosides known to deter insects (*3*). This function of glucosinolates requires their tissue damage–triggered activation

by specialized β-thioglucoside glucohydrolases (TGGs, also called myrosinases) (*4*) compartmentalized either in specialized myrosin cells in the phloem parenchyma (*5*) or in stomata cells (*6*).

Arabidopsis is immune to nonadapted powdery mildew fungi, such as *Blumeria graminis* and *Erysiphe pisi*, that colonize grass and pea species, respectively. During these interactions, fungal pathogenesis is terminated coincident with the switch from surface to invasive growth by two parallel pathways of induced preinvasive defense responses. The *Arabidopsis* PEN1 syntaxin resides in the plasma membrane and forms hetero-oligomeric complexes for vesicle-mediated secretory defense together with the adaptor SNAP33 and endomembrane-anchored VAMP721/722 (*7, 8*). PEN2, a deduced family 1 glycosyl hydrolase (F1GH), and the plasma membrane-resident PEN3 ATP (adenosine triphosphate)–binding cassette (ABC) transporter act in a second path-

[1]Department of Plant Microbe Interactions, Max Planck Institut für Züchtungsforschung, Carl-von-Linné-Weg 10, D-50829 Köln, Germany. [2]Max Planck Institute for Chemical Ecology, Beutenberg Campus, Hans-Knöll-Straße 8, D-07745 Jena, Germany. [3]Centro de Biotecnología y Genómica de Plantas, Universidad Politécnica de Madrid, Campus Montegancedo, E-28223-Pozuelo de Alarcón (Madrid), Spain.

*To whom correspondence should be addressed. E-mail: schlef@mpiz-koeln.mpg.de (P.S.-L.); bednarek@mpiz-koeln.mpg.de (P.B.)
†Present address: Max Planck Institut für Bioanorganische Chemie, Stiftstrasse 34–36, D-45470 Mülheim an der Ruhr, Germany.
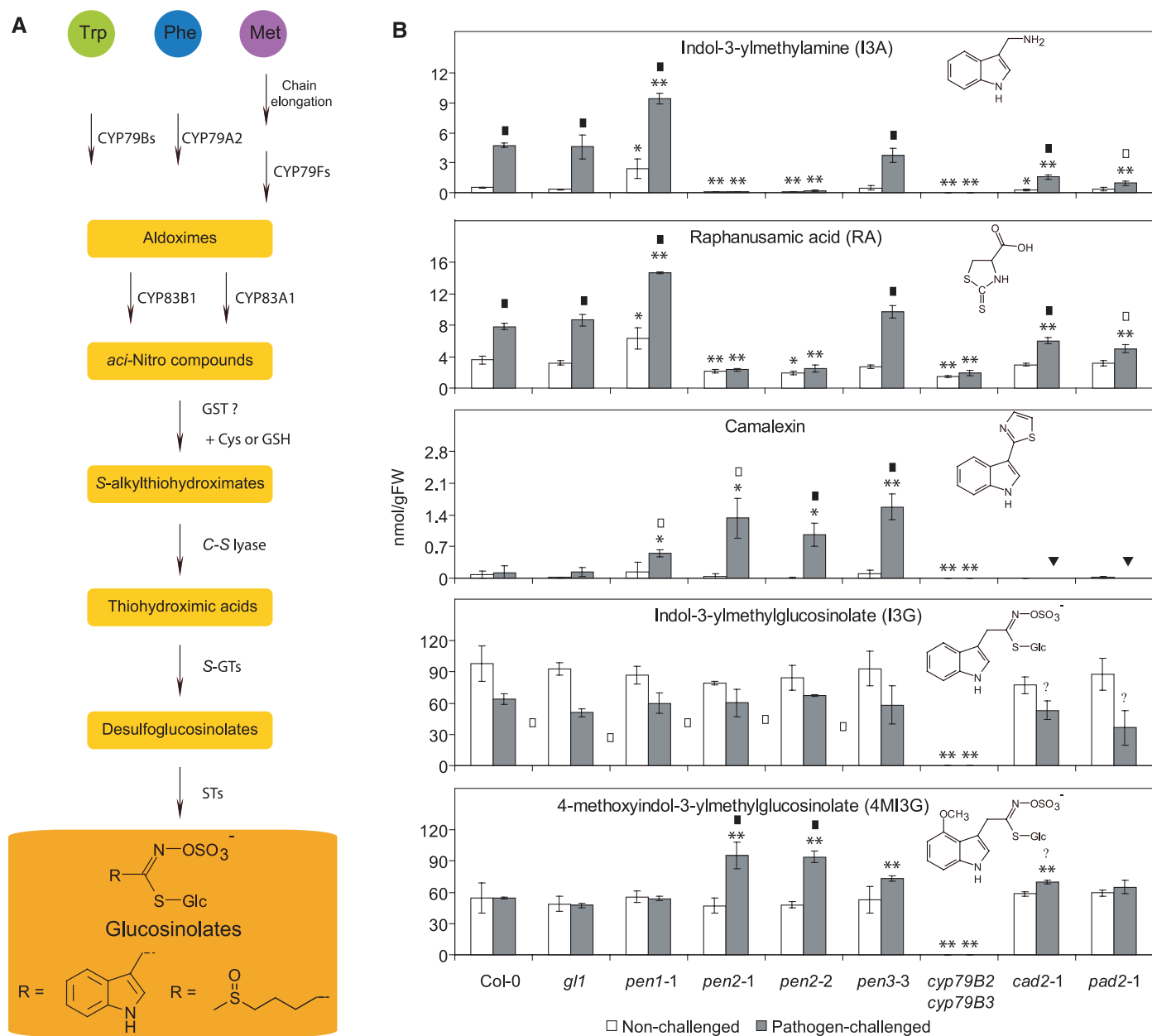
Fig. 1. (**A**) A simplified scheme of glucosinolate biosynthesis in *Arabidopsis*. Structures of the R groups of indol-3-ylmethyl (left) and 4-methylsulfinylbutyl glucosinolate (right) are shown as examples of *Arabidopsis* tryptophan- and methionine-derived glucosinolates, respectively. *S*-GT indicates *S*-glucosyltransferase and ST, sulfotransferase. (**B**) Accumulation of selected secondary metabolites, indicated as nmol/g of fresh tissue weight (FW), in *Arabidopsis* genotypes 16 hours after inoculation with *B. g. hordei* conidiospores. Error bars indicate standard deviations. ■ *P* < 0.005, □ *P* < 0.05 (two-tailed *t* test for pairwise comparisons of nonchallenged and challenged plants). **P < 0.005, *P < 0.05 (comparison of respective wild-type and mutant plants). ▼ variation in camalexin accumulation between experiments. (**C**) Frequency of invasive growth at *B. g. hordei* and *E. pisi* interaction sites on *Arabidopsis* genotypes scored 48 or 72 hours, respectively, after inoculation with conidiospores. Error bars, SD. **P < 0.001, *P < 0.01 (two-tailed *t* test for pairwise comparisons of respective wild-type and mutant plants).

way and have been implicated in the cytoplasmic synthesis and transport of unknown small molecules across the plasma membrane (9, 10). The biochemical pathway underlying PEN2- and PEN3-dependent defense is of particular interest because this pathway restricts the growth of a broader spectrum of pathogens, including the nonadapted oomycete *Phytophthora infestans*, the adapted powdery mildews *Golovinomyces orontii* and *G. cichoracearum*, and the necrotrophic fungus *Plectosphaerella cucumerina* (9, 10). In addition, *PEN2* and *PEN3* were recently shown to be required for the extracellular accumulation of the glucan polymer callose, mediated by the glucan synthaselike enzyme PMR4/GSL5, in response to treatment with a microbe-associated molecular pattern (MAMP) derived from bacterial flagellin (11).

pen2 plants fail to accumulate an indole and a cysteine metabolite. PEN2 is 1 of 42 annotated F1GHs in the *Arabidopsis* Col-0 genome (12). These enzymes usually catalyze the hydrolysis of a β-glycosidic or a thio-β-glycosidic bond between two or more carbohydrates or between a carbohydrate and a noncarbohydrate (so-called aglycone) residue (4, 12, 13). To identify PEN2 candidate substrate(s) and product(s), we performed comparative metabolite profiling experiments with

use of leaf extracts of wild-type strains (Col-0 and *gl1*), *pen1*-1 null mutant, two independent *pen2* mutant lines (*pen2*-1 and *pen2*-2), and *pen3*-3 null mutants (14). These experiments revealed a specific defect in the pathogen (*B. g. hordei*)-inducible accumulation of two compounds in *pen2* tissue: a novel metabolite with spectral properties similar to indole derivatives and a putative cysteine derivative, raphanusamic acid (RA), whose function and biosynthetic origin is unclear (15). We purified the former, and its structure was identified on the basis of mass spectrometry (MS) and nuclear magnetic resonance (NMR) techniques as indol-3-ylmethylamine (I3A) (Fig. 1B and fig. S1) (14). The indole core structure suggested a tryptophan biosynthetic origin. We investigated *cyp79B2 cyp79B3* double mutants defective in the P450 monooxygenase-catalyzed conversion of tryptophan to indole-3-acetaldoxime, a precursor of most known tryptophan-derived metabolites (16, 17). *cyp79B2 cyp79B3* plants fail to accumulate detectable I3A quantities (Fig. 1B), confirming that tryptophan is the biosynthetic I3A precursor. Moreover, the presumed cysteine derivative RA was no longer pathogen-inducible in *cyp79B2 cyp79B3* leaves (Fig. 1B), demonstrating that coaccumulation of structurally unrelated RA and I3A is dependent on an intact tryptophan metabolism.

Arabidopsis PAD2, encoding γ-glutamylcysteine synthetase (γ-ECS), has previously been linked to the biotic stress-induced accumulation of the phytochemicals glucosinolates and camalexin, which require cysteine incorporation into their core structure (18, 19). PAD2 catalyzes the first committed step of glutathione biosynthesis, and *pad2*-1 mutants contain ~20% of the amount of glutathione present in wild-type plants, accumulate reduced amounts of these phytochemicals upon biotic stress, and are susceptible to infection by bacteria and oomycete pathogens, as well as herbivory by generalist insects (18, 19). We examined the impact of the glutathione/cysteine metabolism on the pathogen-induced accumulation of the presumed cysteine derivative RA. In comparison with wild-type and *pen2* plants, both *pad2*-1 and an independent mutant allele, designated *cad2*-1 (18, 20), produced not only intermediate amounts of RA but also of I3A after *B. g. hordei* inoculation (Fig. 1B), suggesting that glutathione is a potential cysteine donor in the biosynthesis of RA and linking RA and I3A accumulation.

We identified three additional tryptophan-derived compounds whose quantities were altered upon pathogen challenge. Camalexin accumulated to higher concentrations in *pen1*, *pen2*, and *pen3* mutants relative to concentrations in wild type (Fig. 1B), suggesting that its inducible biosynthesis is an indirect effect resulting from both elevated *B. g. hordei* entry rates and induction of death of invaded host epidermal cells (9, 21). The other two compounds, according to structure analysis, were indol-3-ylmethylglucosinolate (I3G) and 4-methoxyindol-3-ylmethylglucosinolate (4MI3G) (SOM text). I3G was reduced 16 hours after *B. g. hordei* inoculation, whereas 4MI3G accumulated in *pen2* inoculated leaves at higher quantities than any other line (Fig. 1B).

Tryptophan-derived indolics are essential for pre- and postinvasion defense. Inoculation of *cyp79B2 cyp79B3* mutant plants with nonadapted *B. g. hordei* or *E. pisi* revealed infection phenotypes indistinguishable from those of *pen2* plants, whereas infected *cad2*-1 and *pad2*-1 plants exhibited moderate fungal entry rates between those of resistant wild-type and those of defense-compromised *pen2* plants (Fig. 1C). This suggests that *CYP79B2/B3* and *PAD2* function in preinvasion resistance, revealing a positive correlation between I3A and RA accumulation and plant defense. However, because *cyp79B2 cyp79B3* plants fail to accumulate multiple groups of indole-type secondary products, including camalexin and indole-type glucosinolates (16, 17), we lack demonstration of a direct role of I3A and RA in *Arabidopsis* defense responses. Of note, we detected extensive epiphytic hyphal growth of *E. pisi* on leaves of *cyp79B2 cyp79B3* plants compared with growth on wild-type and *pen2* leaves (fig. S2). We therefore tested the *pad3*-1 mutant (22), which is specifically compromised in camalexin biosynthesis, and a *pen2 pad3* double mutant. *E. pisi* infection phenotypes on *pad3* plants were indistinguishable from that of wild-type, whereas *pen2 pad3* plants
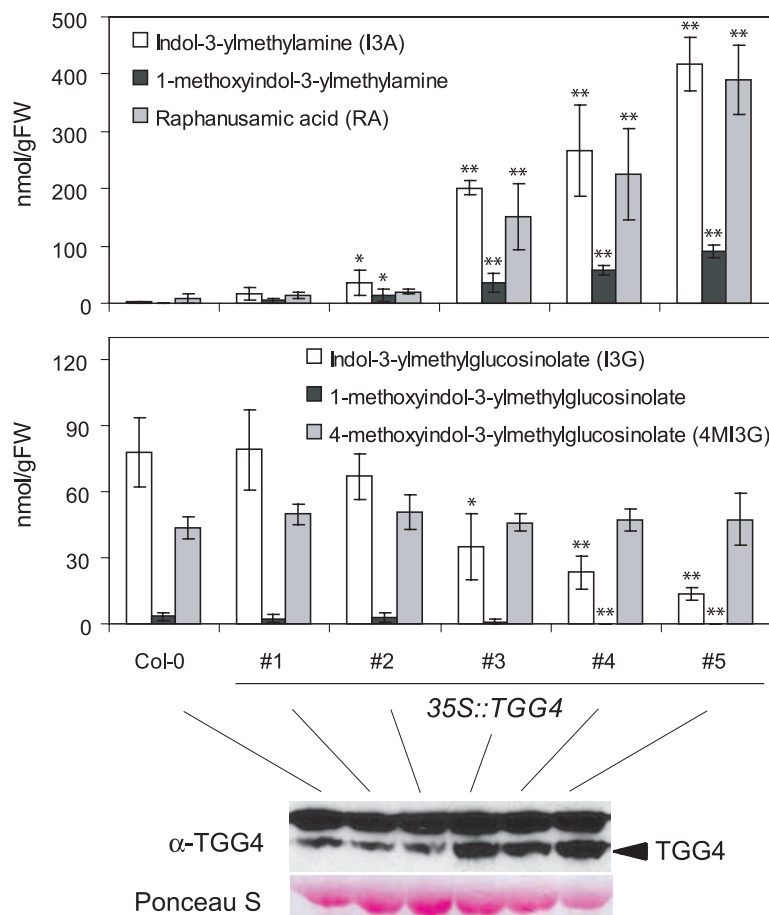
Fig. 2. Accumulation of selected secondary metabolites and immunodetection of TGG4 myrosinase in independent *Arabidopsis* transgenic lines constitutively expressing *TGG4*. Error bars, SD. **$P < 0.001$; *$P < 0.01$ (two-tailed *t* test for pairwise comparisons of Col-0 and respective transgenic plants).

resembled *cyp79B2 cyp79B3* plants in entry rates and epiphytic hyphal growth (Fig. 1C and fig. S2). This suggests that the infection phenotype of *cyp79B2 cyp79B3* plants results from the absence of both PEN2-generated products and camalexin. On the basis of these data, we propose that PEN2 and PAD3 act sequentially during pre- and post-invasive defenses, respectively. This would explain why camalexin amounts are elevated in mutants defective in preinvasion resistance [such as *pen1* and *pen3* (Fig. 1B)], because these plants have a compensatory postinvasive and cell death–associated defense that is lacking in wild type (*9*).

Myrosinase misexpression supports the existence of a novel glucosinolate metabolism pathway. Our data suggest an unexpected role of glucosinolates in fungal defense (Fig. 1B and figs. 1C and S2). We generated *Arabidopsis* lines expressing the root myrosinase *At*TGG4 (*12*, *23*) constitutively. Previously reported in vitro hydrolysis end products of I3G (*24*, *25*) were either undetectable (e.g., indol-3-ylcarbinol) or present at low abundance (e.g., indol-3-ylacetonitrile) in these lines (fig. S3A). Instead, transgenic *35S::TGG4* expressing lines showed a constitutive hyperaccumulation of I3A and RA (Fig. 2). Increasing amounts of both compounds correlated with TGG4 protein abundance and a concomitant depletion of I3G (Fig. 2).

Hyperaccumulation of I3A and RA was independent of PEN2 activity because *At*TGG4 overexpression in the *pen2*-1 background resulted in similar biochemical phenotypes (fig. S3B). Taken together, the metabolite profiles of both pathogen-challenged wild-type plants (Fig. 1B) and *35S::TGG4* lines (Fig. 2) suggest that myrosinase-dependent hydrolysis of glucosinolates occurs in vivo in living plant cells and generate different end products from those reported from studies of in vitro hydrolysis and damage by chewing insects (*24*, *25*). This also suggests that the amine I3A and RA are proxies of in vivo indole glucosinolate metabolism rather than specific markers of PEN2 activity.

We detected 1-methoxyindol-3-ylmethylamine (Fig. 2) (*14*) in *35S::TGG4* plants when looking for structure variants of indole-type and/or methionine-derived aliphatic glucosinolates (a glucosinolate subclass, Fig. 1A) subject to in vivo hydrolysis. We postulated that this molecule could be derived from a low abundance 1-methoxyindol-3-ylmethylglucosinolate in *Arabidopsis* leaves (*26*). Liquid chromatography/mass spectrometry (LC/MS) also revealed the presence of additional amines in extracts from *35S::TGG4* plants that correspond in their side chain structure to *Arabidopsis* aliphatic glucosinolates (fig. S3C) (*14*). These observations suggest that both indole and aliphatic glucosinolates undergo metabolism in vivo with a concomitant buildup of the respective amines.

Amounts of one of the two methoxylated indole glucosinolates, 4MI3G, remained unaffected in tested transgenic lines (Fig. 2), and the corresponding 4-methoxyindol-3-ylmethylamine (4MI3A) was barely detectable by LC/MS (*14*).

PEN2 is an atypical myrosinase. The detection of a novel glucosinolate metabolism pathway in intact tissue together with the identification of I3A and RA as pathogen-inducible and PEN2-dependent metabolites predicted that PEN2 functions as a myrosinase. This was unexpected because the enzyme possesses an acid/base catalyst glutamic acid in its catalytic cleft (Glu[183], E183) (*9*), characteristic for β-*O*-glycosylhydrolases but not myrosinases (*4*, *12*). We heterologously expressed an epitope-tagged fusion protein lacking 64 residues from the C-terminal region, which is possibly critical for in planta subcellular PEN2 localization (*9*). This vector, PEN2Δ-*Strep*, permitted high protein expression in *Pichia pastoris*. Affinity chromatography–purified PEN2Δ-*Strep* (fig. S4A) showed a pH optimum around 6 (fig. S4B) and cleaved in vitro both *S*-glucosides (I3G and 4MI3G) and, at ~10-fold lower maximum reaction rate and ~fivefold lower Michaelis con-

stant, a model *O*-glucoside (4-methyl-umbelliferyl-β-D-*O*-glucoside, 4MUG) (fig. S4C). We tested the in vitro activity of a site-directed mutant (Glu[183]→Asp[183]), PEN2$_{E183D}$Δ-*Strep*, in order to test these molecules as physiologically relevant substrates. The stable, full-length PEN2$_{E183D}$ variant was inactive in vivo because it failed to rescue impaired entry resistance to *B. g. hordei* in the *pen2* background (*9*). Remarkably, PEN2$_{E183D}$Δ-*Strep* failed to convert the glucosinolate I3G but retained β-*O*-glycosylhydrolase activity in the presence of 4MUG (fig. S4, A and C), suggesting that PEN2 acts as myrosinase in vivo and implicating glucosinolate-derived products as antifungal defense compounds. Furthermore, RA was no longer pathogen-inducible in the *cyp79B2 cyp79B3* mutant lines (Fig. 1B) despite the accumulation of aliphatic glucosinolates (*16*), indicating that PEN2 cleaves indole glucosinolates in planta preferentially, if not exclusively.
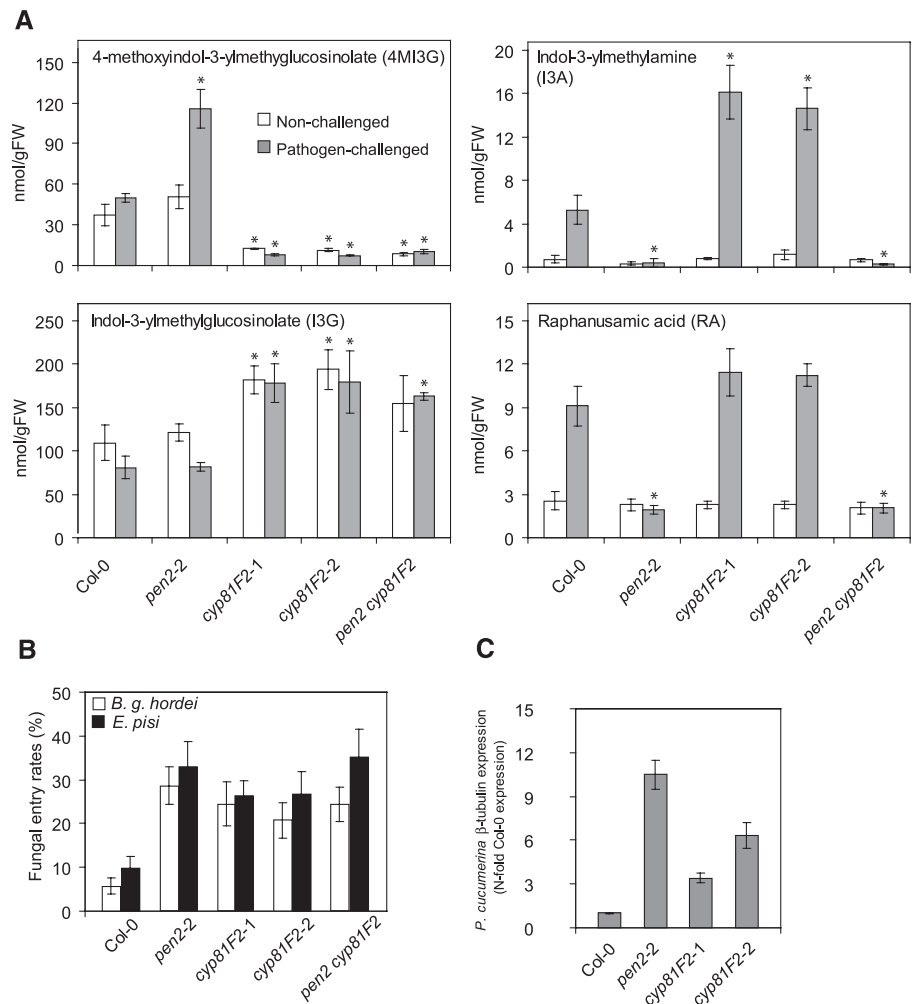
Fig. 3. (**A**) Accumulation of selected secondary metabolites in *Arabidopsis* genotypes 16 hours after inoculation with *B. g. hordei* conidiospores. Error bars, SD; *$P < 0.005$ (two-tailed *t* test for pairwise comparisons of Col-0 and respective mutant plants). (**B**) Frequency of invasive growth at *B. g. hordei* and *E. pisi* interaction sites scored 48 or 72 hours after inoculation. Error bars, SD; all differences between Col-0 and tested mutant lines are significant at $P < 0.001$ (two-tailed *t* test). (**C**) Growth of *P. cucumerina* as determined by real-time quantitative reverse transcriptase polymerase chain reaction of *P. cucumerina* β-tubulin 3 days after inoculation with spores. Error bars, SD; all differences between Col-0 and tested mutant lines are significant at $P < 0.05$ (two-tailed *t* test).

Although amines and RA have not been considered as glucosinolate hydrolysis products to date (*24*, *25*), the myrosinase hydrolysis product of glucosinolate sinigrin, allylisothiocyanate, decomposes in the presence of nucleophilic reagents to an amine (*27*). This and the fact that reduced glutathione is one of the most abundant plant nucleophiles (*28*) suggested a possible metabolic link between I3G and I3A/RA by which glucosinolate-derived isothiocyanate and glutathione form a dithiocarbamate adduct that is later converted to the respective amine and RA (fig. S5A). This pathway is likely because the formation of corresponding adducts occurs (i) nonenzymatically (*29*), (ii) enzymatically, driven by glutathione-*S*-transferases (GSTs) in vitro (*30*), or (iii) in vivo in mammals after consuming glucosinolates or isothiocyanates in Brassicaceae vegetables (*31*).

Biosynthesis and cleavage of 4MI3G is essential for plant defense. It is likely that I3G and 4MI3G are directly metabolically connected as uptake of I3G by detached *cyp79B2 cyp79B3* leaves restores the accumulation of 4MI3G (*32*). If so, then the fungus-induced depletion of I3G

and the concomitant *pen2* mutation-dependent increase in 4MI3G (Fig. 1B) suggest that the latter glucosinolate is critical for fungal defense. We reasoned that conversion of I3G to 4MI3G may involve the hydroxylation of the indole core by cytochrome P450 monooxygenases and that the corresponding gene(s) might be coexpressed with *PEN2*. Microarray data sets (*33*) in *Arabidopsis* identified five P450 monooxygenase genes that coexpressed with *PEN2*, *PEN3*, and *CYP83B1* ($r = 0.4$; the latter gene encodes a P450 monooxygenase required for glucosinolate biosynthesis). Transferred-DNA insertions in the *At5g57220* gene, encoding CYP81F2, showed reduced 4MI3G amounts (Fig. 3A), linking CYP81F2 with 4MI3G biosynthesis. Both *cyp81F2* mutant lines showed impaired entry resistance to *B. g. hordei* and *E. pisi* and were more susceptible to *P. cucumerina* (Fig. 3B and C), reminiscent of the *pen2* infection phenotypes (*9*). We also generated *cyp81F2 pen2* double mutants in which the resistance phenotype was indistinguishable from that in the single mutants (Fig. 3B). This suggests that *CYP81F2* and *PEN2* act in a common pathway. Moreover, although

PEN2 can hydrolyze both unsubstituted and methoxylated indole glucosinolates (fig. S4C), only the compound(s) derived from 4MI3G is important for the restriction of fungal growth. Retained accumulation of I3A and RA in *cyp81F2* plants excludes their direct function in preinvasion resistance. Despite analyses supported with a synthetic reference compound (*14*), we did not detect pathogen-inducible accumulation of 4MI3A (the predicted product derived from 4MI3G). This suggests an alternative biochemical route for the processing of the 4-methoxylated indole dithiocarbamate adduct (Fig. 4A and fig. S5). The structural similarity of this intermediate with the core structure of a major group of Brassicaceae phytoalexins (*34*) supports an already-proposed close metabolic link between these compounds (*35*, *36*) and indole glucosinolates, pointing at them as possible antimicrobial end products of the CYP81F2/PEN2 pathway and as coactivators of MAMP-triggered PMR4/GSL5-dependent callose formation (*11*).

Conclusions. Our study revealed a PEN2-driven glucosinolate metabolism pathway that is fundamentally different from insect interactions with plants in the Brassicaceae family (*24*, *25*). Unlike the passive mode of glycoside activation by myrosinases and other F1GHs (*13*), PEN2-dependent indole glucosinolate hydrolysis is an active process involving directed movement to, and concentration of, the peroxisome associated enzyme to the cell periphery at fungal entry sites (*9*), which likely generates high local concentrations of hydrolysis product(s). Our work questions the specificity of *O*- and *S*-glycosylhydrolases (*4*, *12*) and reveals different glucosinolate end products relative to those produced after insect-mediated tissue destruction (fig. S5A). This discrepancy results most likely from the in vivo conjugation of the glucosinolate hydrolysis product, isothiocyanate, with glutathione to form a dithiocarbamate adduct, which is subject to further processing (Fig. 4A and fig. S5). Because this metabolism pathway occurs only in living cells, the engagement of specific enzymatic activities, or even specialized enzymatic complexes, appears likely (*37*). Moreover, the strict requirement of a particular aglycone structure (4MI3G) in the tested plant-fungus interactions contrasts with the limited structural specificity of glucosinolates in deterring insects (*3*, *32*).

The glucosinolate pathway originates from the biosynthesis of cyanogenic glucosides and most likely was initiated by the appearance of CYP83 enzymes that convert acetaldoximes to reactive *aci*-nitro compounds (Figs. 1A and 4B) (*37*). Because most of the enzymes acting downstream of CYP83s represent classes involved in detoxification, like GSTs, glucosyltransferases, and sulfotransferases (*3*, *19*), the glucosinolate pathway may have evolved from routes triggered by the appearance of toxic CYP83 product(s) (*38*). In parallel or subsequently, a class of F1GHs emerged that is capable of cleaving glucosinolates for insect defense and turnover. However, because the direct

Fig. 4. (**A**) Involvement of tryptophan-derived metabolites in *Arabidopsis* defense against powdery mildews. Components critical for termination of pre- and postinvasive fungal growth are highlighted with blue and orange frames, respectively. The matching structure fragments of the isothiocyanate-glutathione adduct and some of the Brassicaceae phytoalexins are highlighted in red; for detailed structures, see fig. S5B. Dashed frames denote putative metabolites derived from 4MI3G. (**B**) Model for reiterated enzymatic cycles controlling the generation of small toxic molecules and their detoxification in *Arabidopsis*.

products of myrosinase activity are toxic, another detoxification cascade involving glutathione conjugation was required, yielding RA and amines (Fig. 4B). This pathway was most likely later recruited into plant defense against microbial intruders. The relatively recent evolution of PEN2 is supported by its unique exon-intron structure (*12*) and also explains the retention of an ancestral function: cleaving *O*-glucosides (fig. S4). This suggests that also one of the most closely related proteins to PEN2 in *Arabidopsis*, the root-specific PYK10 enzyme (*39*), which restricts colonization by a soil-borne fungus (*40*), may act as a second generation myrosinase. The seven PEN2-like F1GHs in the *Arabidopsis* genome suggests that glucosinolate hydrolysis has been repeatedly engaged in plant defense or glucosinolate turnover and may have given rise to a diverse array of phytochemicals.

References and Notes

1. R. A. Dixon, *Nature* **411**, 843 (2001).
2. J. Tsuji, E. P. Jackson, D. A. Gage, R. Hammerschmidt, S. C. Somerville, *Plant Physiol.* **98**, 1304 (1992).
3. B. A. Halkier, J. Gershenzon, *Annu. Rev. Plant Biol.* **57**, 303 (2006).
4. W. P. Burmeister *et al.*, *Structure* **5**, 663 (1997).
5. E. Andreasson, L. B. Jorgensen, A. S. Hoglund, L. Rask, J. Meijer, *Plant Physiol.* **127**, 1750 (2001).
6. C. Barth, G. Jander, *Plant J.* **46**, 549 (2006).
7. N. C. Collins *et al.*, *Nature* **425**, 973 (2003).
8. C. Kwon *et al.*, *Nature* **451**, 835 (2008).
9. V. Lipka *et al.*, *Science* **310**, 1180 (2005).
10. M. Stein *et al.*, *Plant Cell* **18**, 731 (2006).
11. N. K. Clay, A. M. Adio, Carine Denoux, G. Jander, F. M. Ausubel, *Science* **323**, 95 (2009).
12. Z. Xu *et al.*, *Plant Mol. Biol.* **55**, 343 (2004).
13. A. V. Morant *et al.*, *Phytochemistry* **69**, 1795 (2008).
14. Materials and methods are available as supporting material on *Science* Online.
15. P. Bednarek, B. Schneider, A. Svatos, N. J. Oldham, K. Hahlbrock, *Plant Physiol.* **138**, 1058 (2005).
16. Y. Zhao *et al.*, *Genes Dev.* **16**, 3100 (2002).
17. E. Glawischnig, B. G. Hansen, C. E. Olsen, B. A. Halkier, *Proc. Natl. Acad. Sci. U.S.A.* **101**, 8245 (2004).
18. V. Parisy *et al.*, *Plant J.* **49**, 159 (2007).
19. K. Schlaeppi, N. Bodenhausen, A. Buchala, F. Mauch, P. Reymond, *Plant J.* **55**, 774 (2008).
20. R. Howden, C. R. Andersen, P. B. Goldsbrough, C. S. Cobbett, *Plant Physiol.* **107**, 1067 (1995).
21. D. J. Kliebenstein, H. C. Rowe, K. J. Denby, *Plant J.* **44**, 25 (2005).
22. N. Zhou, T. L. Tootle, J. Glazebrook, *Plant Cell* **11**, 2419 (1999).
23. P. Zimmermann, M. Hirsch-Hoffmann, L. Hennig, W. Gruissem, *Plant Physiol.* **136**, 2621 (2004).
24. A. M. Bones, J. T. Rossiter, *Phytochemistry* **67**, 1053 (2006).
25. M. Burow *et al.*, *Phytochemistry* **69**, 663 (2008).
26. B. L. Petersen, S. X. Chen, C. H. Hansen, C. E. Olsen, B. A. Halkier, *Planta* **214**, 562 (2002).
27. K. Cejpek, J. Valusek, J. Velisek, in *Biologically Active Phytochemicals in Food*, W. Pfannheuser, G. R. Fenwick, S. R. Khokhar, Eds. (Royal Society of Chemistry, Norwich, UK, 2001), pp. 480–484.
28. D. P. Dixon, I. Cummins, D. J. Cole, R. Edwards, *Curr. Opin. Plant Biol.* **1**, 258 (1998).
29. G. Brusewitz *et al.*, *Biochem. J.* **162**, 99 (1977).
30. Y. Zhang, R. H. Kolm, B. Mannervik, P. Talalay, *Biochem. Biophys. Res. Commun.* **206**, 748 (1995).
31. B. Holst, G. Williamson, *Nat. Prod. Rep.* **21**, 425 (2004).
32. J. H. Kim, G. Jander, *Plant J.* **49**, 1008 (2007).
33. T. Obayashi *et al.*, *Nucleic Acids Res.* **35**, D863 (2007).
34. M. S. C. Pedras, Q.-a. Zheng, V. K. Sarma-Mamillapalle, *Nat. Prod. Commun.* **2**, 319 (2007).
35. K. Monde, M. Takasugi, T. Ohnishi, *J. Am. Chem. Soc.* **116**, 6650 (1994).
36. M. S. C. Pedras, D. P. O. Okinyo, *Org. Biomol. Chem.* **6**, 51 (2008).
37. B. S. J. Winkel, *Annu. Rev. Plant Biol.* **55**, 85 (2004).
38. C. H. Hansen *et al.*, *J. Biol. Chem.* **276**, 24790 (2001).
39. A. J. Nagano, Y. Fukao, M. Fujiwara, M. Nishimura, I. Hara-Nishimura, *Plant Cell Physiol.* **49**, 969 (2008).
40. I. Sherameti *et al.*, *Plant J.* **54**, 428 (2008).
41. We thank J. Meier for the TGG4 antiserum and S. Rosahl and L. Westphal for *pen2 pad3* seeds. Partially supported by the Max Planck Chemical Genomics Center, Spanish Ministerio de Educación y Ciencia (MEC; grant BIO2006-00488) and a Ph.D. fellowship (A.S.-V.).

REPORTS

Mott Insulating State in Ultraclean Carbon Nanotubes

Vikram V. Deshpande,[1]* Bhupesh Chandra,[2] Robert Caldwell,[3] Dmitry S. Novikov,[4] James Hone,[2]† Marc Bockrath[1]†

The Mott insulating state is a manifestation of strong electron interactions in nominally metallic systems. Using transport spectroscopy, we showed that an energy gap exists in nominally metallic carbon nanotubes and occurs in addition to the band gap in small–band-gap nanotubes, indicating that carbon nanotubes are never metallic. This gap has a magnitude of ~10 to 100 milli–electron volts and a nanotube radius (*r*) dependence of ~1/*r*, which is in good agreement with predictions for a nanotube Mott insulating state. We also observed neutral excitations within the gap, as predicted for this state. Our results underscore nanotubes' exceptional capabilities for use in studying correlated electron phenomena in one dimension.

According to the quantum theory of solids, materials can be either metallic or band insulators. However, this theory breaks down in metals at half-filling of energy bands, in which strong Coulomb repulsion makes it energetically favorable for electrons to localize, one electron per atomic site, to form a Mott insulator (*1*). This state is known to be antiferromagnetically ordered in higher dimensions and has been observed in a variety of bulk systems, including thin films (*2*), nanobeams (*3*), and optical lattices (*4*). The one-dimensional (1D) analog of this state has no long-range magnetic order and can form a spin liquid with gapped spin excitations (*5*). The presence of a spin gap in some classes of spin liquids is be-

lieved to be related to the emergence of high-temperature superconductivity in cuprate oxides (*6*), motivating a search for such systems. Theoretical work (*7–12*) predicts that carbon nanotubes are a realization of a gapped spin liquid Mott insulator.

Experiments on bulk quasi-1D Mott insulating systems (*5*) typically use chemical doping, which introduces additional disorder. Carbon nanotubes offer the opportunity to study electronic phenomena without interference from disorder by using electric-field doping. Recently, the fabrication of ultraclean nanotube devices (*13*) has facilitated the observation of long-predicted phenomena, such as Wigner crystallization (*14*) in large–band-gap nanotubes, as well as spin-orbit coupling (*15*), and may produce favorable conditions for observing a tunable 1D Mott insulator in an individual nanostructure.

We show that the energy gaps exhibited by carbon-nanotube field-effect devices made from small–band-gap and nominally metallic nanotubes cannot be accounted for using noninteracting electron pictures but agree well with predictions for a spin-liquid Mott insulating state in carbon nanotubes. These finite-sized samples act as quantum dots, and Coulomb peaks corresponding to a single electron or hole pair at the band edges are observable. We tuned the magnitude of the energy gap by applying an axial magnetic field (*16*). By tracking the first electron- and hole-addition

[1]Applied Physics, California Institute of Technology, Mail Stop 128-95, Pasadena, CA 91125, USA. [2]Department of Mechanical Engineering, Columbia University, New York, NY 10027, USA. [3]Department of Applied Physics, Columbia University, New York, NY 10027, USA. [4]Department of Physics, Yale University, New Haven, CT 06511, USA.

*Present address: Department of Physics, Columbia University, New York, NY 10027, USA.
†To whom correspondence should be addressed. E-mail: mwb@caltech.edu (M.B.); jh2228@columbia.edu (J.H.)